Total and differential charge transfer cross sections in He^{2+} + N^{4+} collisions

2001 J. Phys. B: At. Mol. Opt. Phys. 34 L93

(http://iopscience.iop.org/0953-4075/34/4/102)

INSTITUTE OF PHYSICS PUBLISHING JOURNAL OF PHYSICS B: ATOMIC, MOLECULAR AND OPTICAL PHYSICS

J. Phys. B: At. Mol. Opt. Phys. **34** (2001) L93–L98 www.iop.org/Journals/jb PII: S0953-4075(01)19494-0

LETTER TO THE EDITOR

Total and differential charge transfer cross sections in $He^{2+} + N^{4+}$ collisions

K von Diemar[1], F Melchert[1], K Huber[1], R Trassl[1,4], E Salzborn[1], L Opradolce[2] and R D Piacentini[3]

[1] Institut für Kernphysik, Universität Giessen, 35392 Giessen, Germany
[2] Instituto de Astronomía y Física del Espacio (CONICET-UBA), CC 67, Suc 28, 1428 Buenos Aires, Argentina
[3] Instituto de Física Rosario (CONICET-UNR), 2000 Rosario, Argentina

E-mail: Roland.H.Trassl@strz.uni-giessen.de

Received 28 November 2000

Abstract

Charge transfer in the collision system $He^{2+} + N^{4+}$ has been investigated both theoretically and experimentally for centre-of-mass energies between 8 and 200 keV. The theoretical calculations of the collision process have been carried out in the semi-classical impact parameter eikonal approach expanding the electronic wavefunction in a multi-state molecular-orbital basis with translation factors. The measurements of the charge-transfer cross sections were performed at an ion–ion *crossed-beams* experiment. Good agreement between the calculations and the experimental results for both total and differential cross sections is obtained.

Charge transfer in ion–ion collisions is a fundamental process in all types of plasmas. Whereas dense plasmas obey the laws of equilibrium thermodynamics, most laboratory as well as astrophysical plasmas are far away from the equilibrium. For the modelling of these non-equilibrium plasmas the knowledge of the fundamental atomic processes, e.g. ion–ion collisions, is essential. Further motivation arises from a basic research point of view. While charge exchange in pure one-electron systems seems to be fairly well understood (see e.g. [1]), only a few experimental and even less theoretical data are available for collision systems involving more than one electron.

In this letter, we report on the theoretical and experimental investigation of the collision reaction

$$He^{2+} + N^{4+}\ (1s^2 2s) \rightarrow He^{+}(nl) + N^{5+}\ (1s^2). \tag{1}$$

In this quasi-one-electron system the nuclear potential for the active 2s electron is screened by the two inner K-shell electrons. Therefore, this collision system is very appropriate for the validity test of one-electron theories.

[4] Corresponding author.

0953-4075/01/040093+06$30.00

Besides the *total* cross section for charge exchange analysed in this letter, we present for the first time *absolute differential* cross section data for the quasi-one-electron system He^{2+}/N^{4+}, which will test the theoretical description of this low-energy ion–ion collision in more detail.

The theoretical treatment of the charge transfer process (1) is performed within the semi-classical impact parameter eikonal approximation, using a molecular expansion that includes common translation factors to take into account the momentum transfer problem. Previous calculations with a similar approach (total cross sections for charge transfer in the iso-electronic He^{2+}/C^{3+} system [2]) are consistent with both experimental and theoretical data obtained by Melchert and co-workers [3]. In this letter, the experimental data were obtained using the same *crossed-beams* technique described below, whereas the calculations were performed using the semi-classical impact parameter method with an atomic-orbital expansion.

The collision system is described as a quasi-molecular ion, $(HeN)^{6+}$, consisting of one active electron e^- and two cores—the He^{2+} nucleus and the N^{5+} $(1s^2)$ inert ion. For the relative core motion we assume straight-line trajectories. Test calculations have been done using a curved trajectory [4] in order to analyse its influence. The integrated cross sections do not show a significant difference compared to the straight-line case over the entire energy range.

For the time-dependent electronic wavefunction expansion, we used eigenfunctions of the Born–Oppenheimer electronic Hamiltonian (H_{el}) of the molecular ion $(HeN)^{6+}$ multiplied by a common phase factor, as has been described elsewhere [5]. To express H_{el} we used a model potential approach [6], taking from [7] the effective potential that represents the electrostatic interaction between the active electron and the N^{5+} $(1s^2)$ core.

The diagonalized Hamiltonian H_{el}, dynamic couplings and common translation factor matrix elements were obtained in the way described by Gargaud and co-workers [8, 9]. The relevant electronic adiabatic potential energy curves for Σ and Π symmetries are shown in figure 1. At large inter-core distances the molecular energies asymptotically match those of the states of separated ions, indicated in the right part of the figure. In the experimental conditions considered here, the collision entry channel is represented by the Σ_1 molecular state. The lowest capture channel is the Σ_3 state, which, at large inter-core distances, correlates with He^+ $(1s) + N^{5+}$ $(1s^2)$. The study of non-adiabatic couplings between molecular states and energetic considerations suggest that the probability flux into the Σ_3 state should account by itself for the experimental cross sections of the charge transfer process.

A similar situation was found for the electron capture process into the ground state of He^+ in He^{2+}/C^{3+} collisions, where the basic capture mechanism was coincidently identified by theoretical calculations and kinematic analysis of the experimental results [2,3]. The molecular structures of both systems are not directly related and no simple relationship can be established between the corresponding cross sections. However, we can predict a lower cross section for the present case since the change in internal energy is greater than in the He^{2+}/C^{3+} system. The molecular orbitals, correlated to the 2p state and the $n = 3$ shell of N^{4+} at large distances, have also been taken into account conforming a nine-state basis set, namely Σ_1 to Σ_6 and Π_1 to Π_3.

Removing the usually small quadratic term in the radial velocity from the system of coupled-channel differential equations we used the code PAMPA [10] in order to obtain the electronic transition amplitudes. The total and differential cross sections for charge transfer are evaluated using the explicit expressions given in [11] by integrating over all significant values of impact parameters. The results of the calculations are compared with the experiment in figures 2 and 4, respectively.

The *crossed-beams* technique employed for the experimental investigation of reaction (1) has been described in full detail earlier [12]. Here, only a short description of the experiment

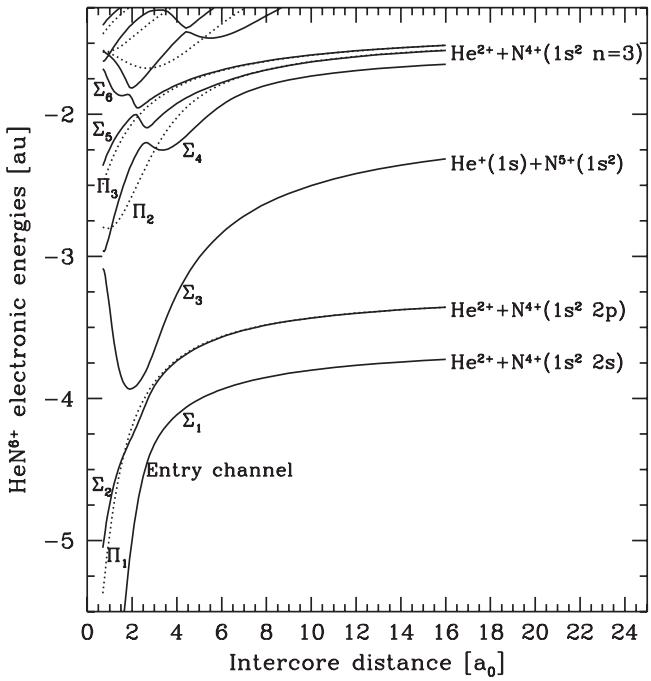

Figure 1. Relevant electronic energy curves of the $(HeN)^{6+}$ molecular ion as a function of the inter-core distance. Solid curves: Σ states; dotted curves: Π states.

will be given. The N^{4+} ions are produced in a 5 GHz ECR ion source and accelerated with a voltage of 7.5 kV. After focusing, the desired mass-to-charge ratio is selected in a 90° analysing magnet and after collimation to typically $1.5 \times 1.5\,mm^2$ the beam enters the interaction chamber. Here, shortly before the interaction at an angle of 17.5°, two electrostatic deflectors clean the ion beam from impurity ions which were produced in collisions with residual gas molecules on its path through the beam line.

In the second beam line, the He^{2+} ions are produced on a high voltage terminal. Here, only limited space and electrical power are available and therefore an all-permanent magnet 10 GHz ECR ion source is used. After extraction and focusing, the ion beam is accelerated with voltages of up to 200 kV, mass-to-charge analysed by a magnet and collimated. We used the $^3He^{2+}$ isotope to avoid contaminations of the primary beam by molecular H_2^+ ions, which have virtually the same mass-to-charge ratio as $^4He^{2+}$ ions. This beam also passes an electrostatic cleaning deflector before intersecting the N^{4+} ion beam at ultra-high vacuum of typically 5×10^{-11} mbar.

After the ion–ion collision, the reaction products remain within their primary ion beams due to the low momentum transfer during the reaction. They are then separated from the parent beams by the use of electrostatic analysers. The reaction products are counted in single-particle detectors whereas the primary ion beams are measured in Faraday cups. Since both reaction products are generated simultaneously and since their flight times from the beam intersection to the detectors are fixed, the corresponding output pulses of single particle detectors show a fixed time delay in the case of true ion–ion signals, whereas there is no time correlation between background events. Hence, time-to-amplitude-converter spectra display a sharp peak produced by ion–ion collisions on top of a flat background due to random coincidences; details

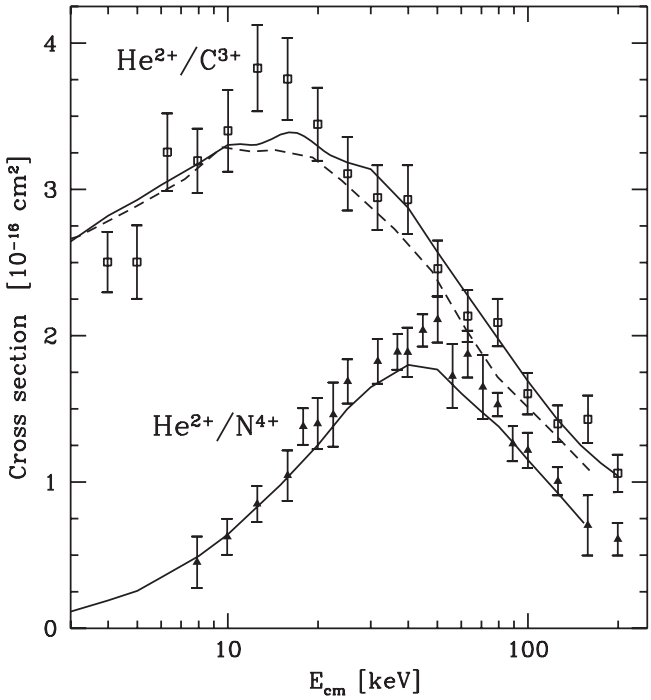

Figure 2. Total cross sections for the single-charge transfer in collisions between $^{3}He^{2+}$ nuclei and $^{14}N^{4+}$ lithium-like ions; triangles, experiment; solid curve, present calculation including nine states. For comparison also shown here are the data obtained in the study of the isoelectronic $^{3}He^{2+}$ + $^{13}C^{3+}$ system; squares, experiment [3]; dashed curve, atomic-orbital theoretical calculations [3]; solid curve, molecular-orbital results [2].

Table 1. Typical experimental parameters during the cross section measurements. E_{FB}, E_{SB}, I_{FB}, I_{SB}, N_{FB}, N_{SB} denote the laboratory energies, ion currents and detector count rates in the 'fast' beam (FB) and 'slow' beam line (SB). R is the coincidence signal rate and t the actual measurement time.

E_{cm} (keV)	E_{FB} (He^{2+}) (keV)	E_{SB} (N^{4+}) (keV)	I_{FB} (nA)	I_{SB} (nA)	N_{FB} (s^{-1})	N_{SB} (s^{-1})	R (s^{-1})	t (s)
15.9	45.4	30	54.0	34.6	6 500	80	0.11	1859
63.1	124.0	30	108.6	38.2	9 300	95	0.50	1130
158.4	264.6	30	164.0	32.8	10 800	2200	0.33	2060

of this technique are discussed in [13]. Table 1 shows some typical experimental parameters as they were used for the measurement of the total cross sections for three different centre-of-mass energies.

The measured total cross sections for charge transfer are shown in figure 2 as a function of the centre-of-mass energy. Although the theoretical results continue to decrease monotonically like the measured data in the upper range of the impact energies investigated, we are not presenting our calculations above 150 keV, since the employed molecular approximation does not take into account the possible influence of the ionization process at higher impact energies.

In order to measure angular-differential cross sections, the scattering distribution of the He^{+} reaction products in the high-energy beam line was detected on a position-sensitive channelplates detector. The extraction of an angular-differential cross section requires the

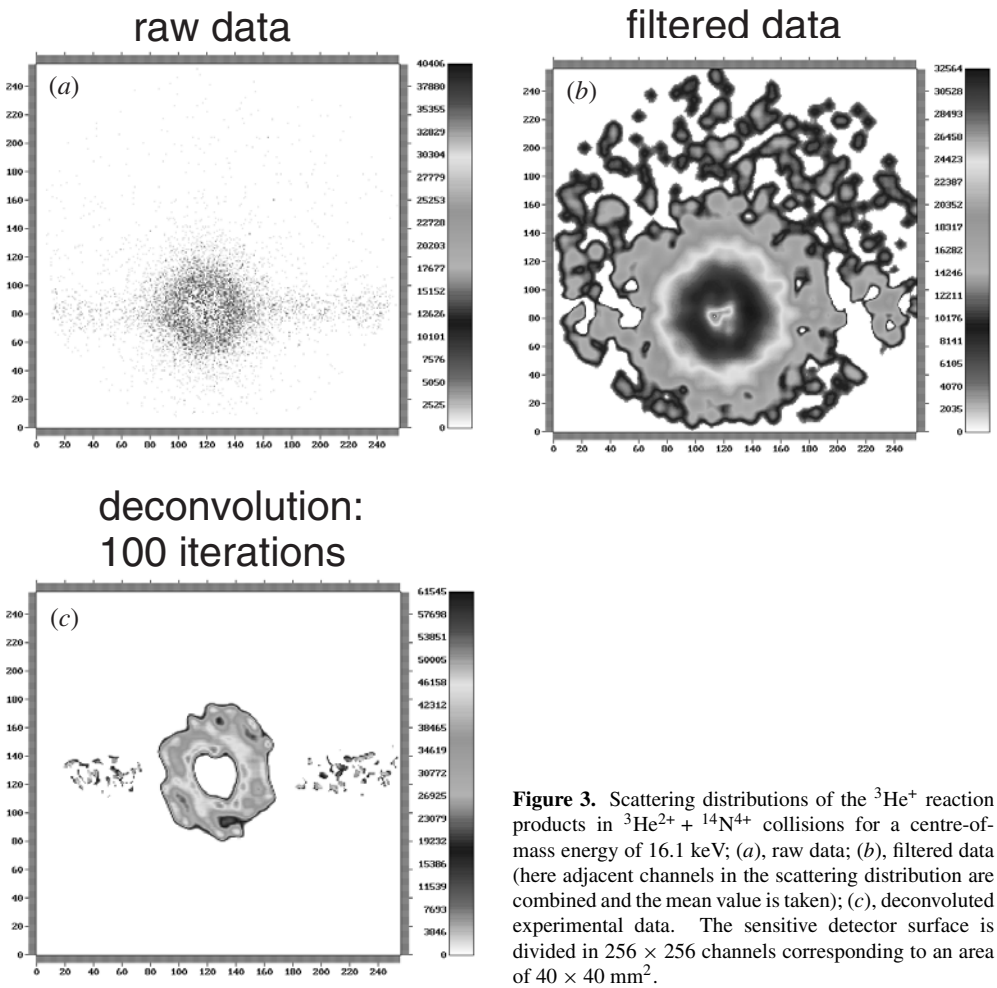

Figure 3. Scattering distributions of the $^3He^+$ reaction products in $^3He^{2+}$ + $^{14}N^{4+}$ collisions for a centre-of-mass energy of 16.1 keV; (*a*), raw data; (*b*), filtered data (here adjacent channels in the scattering distribution are combined and the mean value is taken); (*c*), deconvoluted experimental data. The sensitive detector surface is divided in 256 × 256 channels corresponding to an area of 40 × 40 mm^2.

transformation into the centre-of-mass system using the *crossed-beams* kinematics as well as the appropriate knowledge of the primary beam profile. This primary ion beam profile broadens the scattering distribution and smears out structures. Hence, the measured scattering distribution was deconvoluted from the primary beam profile [14]. The scattering distribution for a centre-of-mass energy of 16.1 keV is shown in figure 3. Integration of the scattering distribution leads to the angular-differential cross section shown in figure 4, where the magnitudes are referred to the centre-of-mass reference frame.

The deconvoluted data for scattering angles up to 1.8° show an oscillatory structure including several maxima and minima, starting with a minimum in forward direction. Figure 4 also compares the experimental data with the present semi-classical eikonal calculations, showing good agreement in the middle range of observed scattering angles. In particular the values for the principal and the two following maxima at low scattering angles are in quantitative agreement with the calculations within the experimental error. It must be pointed out that a calculation made with a simple four-state basis set—Σ_1, Σ_2, Π_1 and Σ_3—reproduces rather well the oscillation pattern at low angles (up to about 0.6°) but starts to be out-of-phase for larger angles.

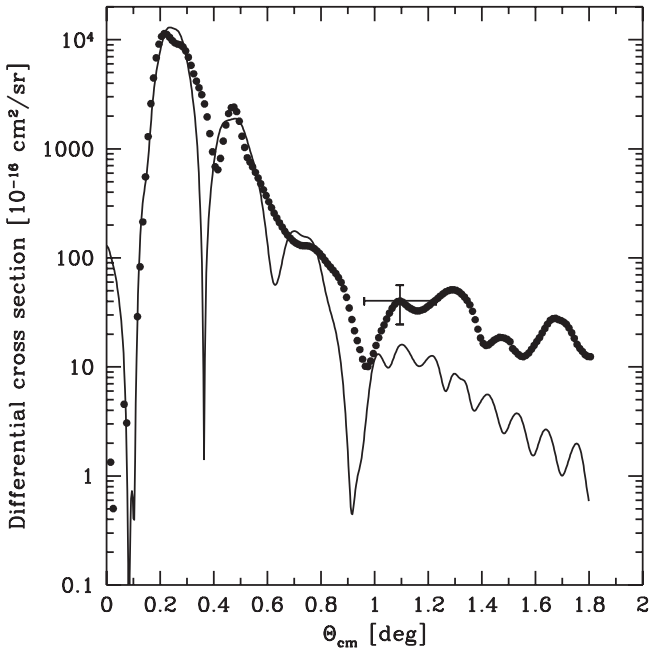

Figure 4. Angular-differential cross section (in absolute values) for the charge transfer process $^3He^{2+} + {}^{14}N^{4+} \rightarrow {}^3He^{+} + {}^{14}N^{5+}$ for a centre-of-mass energy of 16.1 keV; solid circles, deconvoluted experimental data; solid curve, present theoretical calculations. Typical error bars are shown for a scattering angle of 1.1°. These values decrease for lower angles whereas they are slightly bigger at larger angles.

In conclusion, we have presented in this letter, measurements of the total as well as the differential cross sections for the single-charge transfer in $He^{2+} + N^{4+}$ collisions that are reasonably well described by the eikonal impact-parameter method, based on a nine-state quasi-one-electron molecular-orbital expansion.

References

[1] Kruedener S, Melchert F, von Diemar K, Pfeiffer A, Huber K, Salzborn E, Uskov D B and Presnyakov L P 1997 *Phys. Rev. Lett.* **79** 1002
[2] Opradolce L, McCarroll R and Piacentini R D 1997 *Nucl. Instrum. Methods* B **132** 302
[3] Melchert F, Meuser S, Kruedener S, Pfeiffer A, von Diemar K, Salzborn E, Sidky E and Lin C D 1997 *J. Phys. B: At. Mol. Opt. Phys.* **30** L697
[4] Piacentini R D and Salin A 1976 *Comput. Phys. Commun.* **12** 199
[5] Opradolce L, Benmeuraiem L, McCarroll R and Piacentini R D 1988 *J. Phys. B: At. Mol. Opt. Phys.* **21** 503
[6] Bottcher C and Dalgarno A 1974 *Proc. R. Soc.* A **340** 187
[7] Gargaud M and McCarroll R 1985 *J. Phys. B: At. Mol. Phys.* **18** 463
[8] Gargaud M, Hanssen J, McCarroll R and Valiron P 1981 *J. Phys. B: At. Mol. Phys.* **14** 2259
[9] Gargaud M, McCarroll R and Valiron P 1987 *J. Phys. B: At. Mol. Phys.* **20** 1555
[10] Gaussorgues C, Piacentini R D and Salin A 1975 *Comput. Phys. Commun.* **10** 223
[11] Piacentini R D and Salin A 1977 *Comput. Phys. Commun.* **13** 57
[12] Meuser S, Melchert F, Kruedener S, Pfeiffer A, von Diemar K and Salzborn E 1996 *Rev. Sci. Instrum.* **67** 2752
[13] Rinn K, Melchert F and Salzborn E 1985 *J. Phys. B: At. Mol. Phys.* **18** 3783
[14] Kruedener S 1995 *Proc. 19th Int. Conf. on the Physics of Electronic and Atomic Collisions (Whistler, Canada, 1995) (AIP Conf. Proc. vol 360)* ed L J Dube, J B A Mitchell, J W McConkey and C E Brion (New York: AIP) p 677